MECHANICAL PROPERTIES OF AL THIN FILM MEASURED BY TWO DIFFERENT METHODS

I. Kuběna[1,2], T. Kruml[1]
[1] Institute of Physics of Materials, Zizkova 22, Brno, Czech Republic
[2] Institute of Materials Science and Engineering, Brno Universtity of Technology, Czech Republic

Received 28.07.2011
Accepted 23.09.2011

Corresponding author: Ivo Kuběna, Institute of Physics of Materials, Zizkova 22, Brno, Czech Republic. kubena@ipm.cz

Abstract
Mechanical properties of an aluminium thin film were measured by microcompression and indentation tests. The microcompression technique combines preparation of specimens using focused ion beam (FIB) and compression test by a nanoindeter device. Cylindrical specimens were prepared by focused ion beam milling. The height of cylindrical specimens was about 2 μm and their diameter about 1,3 μm. The load and displacement were continuously measured during tests. The stress-strain curves were obtained in two representations. Stresses of the first plastic bursts were determined in both representations. Hardness and Young modulus were measured by indentation test using continuous stiffness method. Representative values of thin film were calculated.

Keywords: thin films, focused ion beam, aluminium, nanoindentation

1 Introduction

Mechanical properties of thin films are generally not easy to be measured. The indentation technique continuously measuring force acting on the specimen and displacement of the indenter is the most popular method. It can be distinguished between nanoindentation and microindentation according to the accuracy and applied loads of the testing device. This method is easy to carry out and a set of material parameters can be measured, nevertheless this method is not suitable for determining of plastic properties of thin films such as yield stress, ultimate stress or strain hardening coefficient [1].

Tensile test is the most suitable method for measuring of plastic properties of bulk materials. Unfortunately, the preparation of specimens from a thin film for tensile test is extremely difficult. For a successful test, the thin film must be separated from the substrate without any damage and the film itself cannot contain defects otherwise the film is fractured before its plastic deformation. There are only rare attempts to perform these experiments in the literature [2-4]. Another possibility is so called bulge test. In this method, the thin film is prepared as a membrane, the gas pressure grows on one side of the thin film and the deflection is measured on the other side [5-7]. The dependence of deflection of thin film on gas pressure can be recalculated to biaxial tensile curve with stress-strain coordinates. The preparation of specimens is also complicated; therefore this method is used only rarely.

Recently, mechanical tests at microscale become more accessible due to commercial availability of focused ion beam (FIB) allowing precise removing of the material and nanoindentation

facilities. Prof. Dimiduk's group was first to carried out mechanical test combining a preparation of specimens using FIB and their subsequent deformation using nanoindenter, so called microcompression test [8]. This technique was used for study of various materials [9-12]. Specimens, referred as pillars, were prepared on polished surface of bulk material and they had a cylindrical geometry. The determination of the effect of specimen size on mechanical behaviour of tested specimen was the main goal of this experiment. The strong increase of yield stress was found in specimens with diameter smaller than 1 μm. A possible explanation for this strengthening is the concept of hardening by dislocation starvation. It means that there are no movable dislocations in such small volume; therefore yield stress is determined by stress which is needed for activation of dislocation sources and not by stress necessary for moving of dislocations as is usual in bulk materials [13].

2 Experiment

The studied material is a thin film of Al – 1,5 wt. % Cu of chemical composition and 2,06 ± 0,05 μm of thickness. The Al film was composed of relatively large grains with the average diameter in the plane parallel to the film surface of 3,8 ± 0,3 μm. Such large grains are a consequence of a relatively high substrate temperature during deposition (340 °C). The EBSD analysis showed a very strong preferential <111> orientation of the normal to the film surface. The film was deposited on <100> Si monocrystalline wafer. In between the wafer and the film, an intermediate W-10%Ti layer was present. The sandwich was prepared on Varian 3190 sputtering system at the ON Semiconductor company.

The microcompression specimens (pillars) were prepared in the Quanta 3D FEG DualBeam™ and Tescan Lyra 3 FEG microscopes. The aim was to obtain a perfect cylindrical specimen with a diameter of 1,3 μm and their height is determined by film thickness. Pillars were produced in centers of large grains, to ensure that the whole pillar is single crystalline. The FIB milling procedure was optimized so that the final shape of the Al part of the pillar is as close to the perfect cylinder as possible.

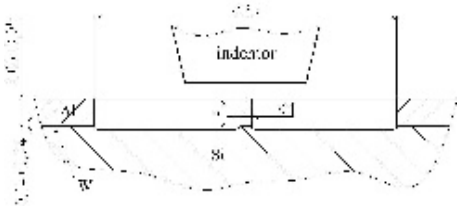

Fig.1 Scheme of microcompression experiment, dimensions in μm.

The diameter of the removed zone around the pillar was chosen to be 25 μm, to ensure that the nanoindenter tip will not touch any other object except the pillar. Flat diamond tip with the diameter of 10 μm was used (see schematics in **Fig. 1**). During the deformation, it was ensured that the face of the flat punch was parallel to the upper face of pillars. At the onset of the deformation, pillars were therefore loaded in pure compression. Micro-compression tests were carried out at nominal constant loading rate of 0,001 mNs^{-1}.

Continuous stiffness measurement technique [14] was used for measuring of indentation modulus and hardness as function of indentation depth using the MTS Nanoindeter XP. The maximum indentation depth was chosen as 2 μm. It is known that measured values of indentation modulus and hardness depend on indentation depth, especially in the case of thin

films deposited on a substrate. Representative values of Al thin film were determined at a plateau which was found in dependences of indentation modulus and hardness on indentation depth. The Berkovich tip geometry was used.

3 Results and discussion

3.1 Microcompression tests

The pillar which was prepared using optimised process is shown in **Fig. 2**. Obviously, the pillar approaches the geometry of a perfect cylinder quite well. The tapper angle is only about 3 degrees, substrate around pillar is also partially removed and substrate geometry around the pillar is not too rough. The pillar after microcompression test is shown in **Fig 3**. The obvious slip bands were produced during plastic bursts during deformation.

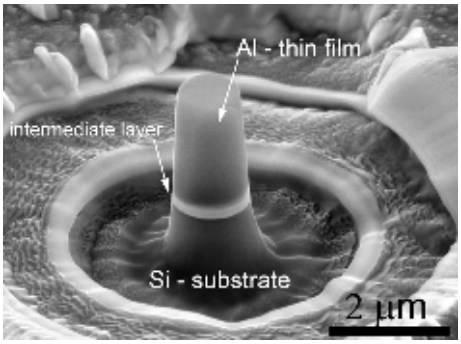

Fig.2 The microcompression pillar before deformation

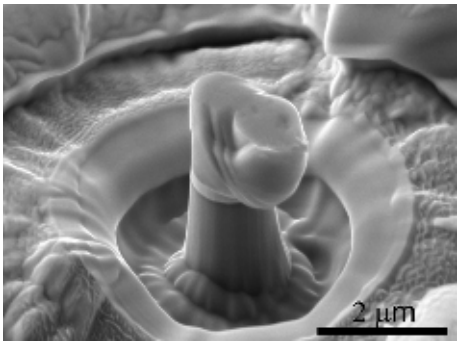

Fig.3 The microcompression pillar after deformation

The displacement of the nanoindenter and applied force were continuously measured during experiment. These quantities were recalculated in engineering stress and strain coordinates by standard equations $\sigma = F / S_0$ and $\varepsilon = \Delta l / l_0$, where l_0 is the initial height of specimen (equal to the thickness of thin film) and S_0 is the initial cross-section. Actually, compression tests were carried out on single crystals, therefore results strongly depend on crystallographic orientation of pillars. The crystallographic orientation was measured by EBSD following by determination of Schmid factor m of the primary slip system. Subsequently, it was possible to recalculate σ–ε coordinates to τ–γ coordinates by equations $\tau = \sigma.m$ and $\gamma = \varepsilon / m$. An example of microcompression curve in both representations is shown in **Fig 4**. It should be noticed that the nanoindentor controls the test and measures the data precisely, although displacement was in the range of *nm* and force in *mN*. Obviously, the shape of the microcompression curve in **Fig. 4** is completely different than typical stress-strain curve for bulk materials. The deformation behaviour of the pillar consisted of events of rapid plastic jumps called plastic bursts connected by stages of elastic deformation. At first, stress increases and pillars are deformed only elastically. After reaching stress necessary for activation of a dislocation source, tens or hundreds of dislocations loops glide through pillar and they disappear on free surface of the pillar. It results in plastic bursts and in fast deformation of the pillar as long as the dislocation source is active. When the dislocation source is exhausted, pillar is deformed again only elastically until other dislocation source is activated. Such explanation of the shape of the microcompression stress-strain curve is generally accepted [15]. The strain hardening was not observed.

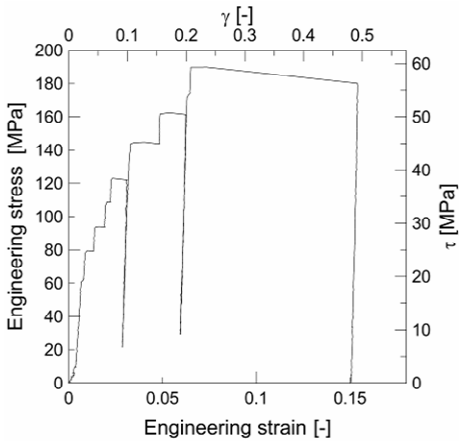

Fig.4 An example of microcompression curve in σ–ε and τ–γ representations.

Due to inability of tungsten alloys and silicon to deform plastically at room temperature, it can be supposed that all plasticity originate from tested Al film so that plastic properties of the Al thin film are measured. The stress at the first plastic burst was determined to be equal 129 ± 44 MPa. Subsequently stress was recalculated to shear stress using Schmid factor, because the plastic behaviour of pillar strongly depends on its crystallographic orientation. The shear stress τ at first plastic bursts was determined as 44 ± 13 MPa. This recalculation decreases the variance of measured data significantly.

3.2 Indentation tests

Two examples of the variation of hardness with displacement of the nanoindentor tip into surface of the thin film are shown in **Fig. 5** and **Fig. 6**. A plateau can be found on that curve in the interval of 150 – 400 nm of indentation depth representing hardness of thin film, see **Fig. 5**. The measured hardness increases with indentation depth because of increasing effect of the substrate. Hardness of the Al thin film was determined by analyzing about 20 experimental curves as 0,71 ± 0,08 GPa.

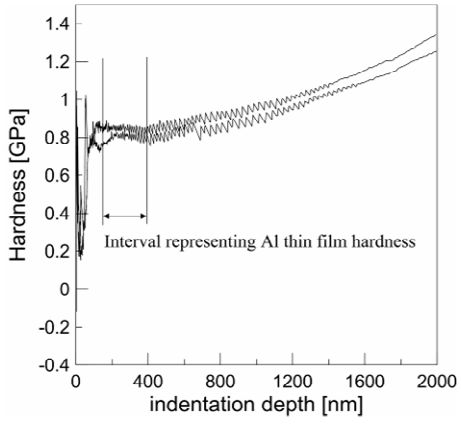

Fig.5 Hardness as a function of indentation depth

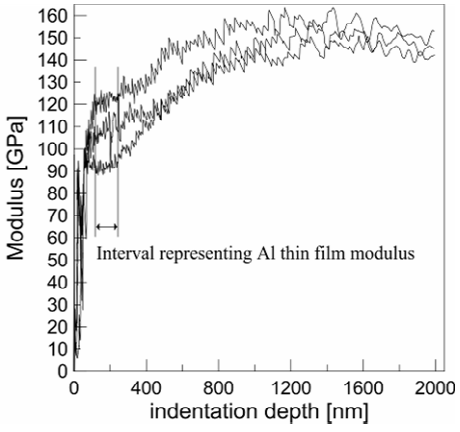

Fig.6 The dependence of indentation modulus on indentation depth

Three examples of the dependence of the indentation modulus E_{ef} on displacement into surface (indentation depth) is shown in **Fig. 6**. There is also strong dependence of indentation modulus on indentation depth due to influence of substrate. The plateau was also found in Fig. 6, nevertheless this plateau occurs in shorter interval of indentation depth (150 – 250 nm) than in case of hardness measurement. The indentation modulus was determined as 102 ± 12 MPa. The Young modulus of thin film can be calculated by equation (1) given in [1]:

$$E_{Al} = \frac{1-\upsilon_{Al}^2}{\frac{1}{E_{ef}} - \frac{1-\upsilon_{in}^2}{E_{in}}} \tag{1}$$

where ν_{Al} and ν_{in} are Poisson ratios of Al and indenter, respectively, and E_{Al}, E_{in} and E_{ef} are Young modulus of thin film, of the indenter and the indentation modulus, respectively. The properties of diamond indenter were found in the literature: E_{in} = 1141 GPa and ν_{in} = 0,07 [1] and Poisson ratio of Al was reported to be equal to be 0,347 [16]. The Young modulus was calculated using these parameters as E_{Al} = 98,6 ± 12,7 GPa. This value is a bit higher than the E for bulk Al ≅ 70 GPa [10]. The tested Al film is strongly textured with preferential <111> orientation parallel to the surface normal. In anisotropic cubic crystal, E of the <111> orientation is higher. Therefore it can be expected that E_{Al} measured on single crystalline specimen with orientation close to <111> will be higher than the average value. Another effect which may increase the measured value of E_{Al} is the influence of the material pushed above the initial surface, so called pile-up [1].

4 Conclusions

Results of this work can be summarised as follows:

- The compression curves in σ–ε representation were obtained during successful compression tests of specimens with size in μm range. The stress of the first plastic burst was determined as 129 ± 44 MPa
- The compression curves were recalculated to τ–γ coordinates using Schmid factor of primary slip system. The shear stress of the first plastic burst was determined as 44 ± 13 MPa.
- Hardness and Young modulus as function of indentation depth were measured by nanoindentation technique using continuous stiffness measurement mode. A plateau was found on the curves representing properties of thin film. The following properties were determined: H = 0,71 ± 0,08 GPa, E_{ef} =102 ± 12 MPa and E_{Al} = 98,6 ± 12,7 MPa.

Acknowledgements

The financial support of the FEI company grant and the Academy of Sciences of the Czech Republic (AV0Z 20410507) is acknowledged.

References

[1] W. C. Oliver, G. M. Pharr: Journal of Material Research, Vol. 7, 1992, p. 1564-1583.
[2] Y.-W. Cheng, D. T. Read, J. D. McColskey, J. E. Wright:Thin Solid Films, Vol. 484, 2005, 426-432.
[3] F. R. Brotzen, C. T. Rosemayer, R. J. Gale: Thin Solid Films, Vol. 166, 1988, p. 291-298.

[4] J.-S. Bae, C.-S. Oh, J.-E. Nam, J.-K. Lee, H.-J. Lee: Current Applied Physics, Vol. 9, 2009, p. 107-109.
[5] M. Cieslar, V. Oliva, A. Karimi, J.-L. Martin: Materials Science and Engineering A, Vol. 387-389, 2004, p. 734-737.
[6] M. Cieslar, V. Oliva, A. Karimi, J.-L. Martin: Journal of Alloys and Compounds, Vol. 378, 2004, p. 312-315.
[7] A. Karimi, O. R. Shojaei, T. Kruml, J.-L. Martin: Thin Solid Films, Vol. 308-309, 1997, p. 334-339.
[8] M. D. Uchic, D. M. Dimiduk: Materials Science and Engineering A, Vol. 400-401, 2005, p. 268-278.
[9] J. R. Greer, W. C. Oliver, W. D. Nix: Acta Materialia, Vol. 53, 2005, p. 1821-1830.
[10] J. R. Greer, C. R. Weinberger, W. Cai: Materials Science and Engineering A: Vol. 493, 2008, p. 21-25.
[11] J.-Y. Kim, J. R. Greer: Acta Materialia, Vol. 57, 2009, p. 5245-5253.
[12] D. Jang, C. T. Gross, J. R. Greer: International Journal of Plasticity, Vol 27, 2011, p. 858-867.
[13] W. D. Nix, J. R. Greer, G. Feng, E. T. Lilleodden: Thin Solid Films, Vol. 515, 2007, p. 3152-3157.
[14] X. Li, B. Bhushan: Materials Characterization, Vol. 48, 2002, p. 11-36.
[15] K. S. Ng, A. H. W. Ngan: Acta Materialia, Vol. 56, 2008, p. 1712-1720.
[16] J. P. Hirth, J. Lothe: Theory of Dislocations, Wiley, New York, 1982.